ACS Catalysis

Letter

pubs.acs.org/acscatalysis

Exploring Low-Temperature Dehydrogenation at Ionic Cu Sites in Beta Zeolite To Enable Alkane Recycle in Dimethyl Ether Homologation

Carrie A. Farberow,[†] Singfoong Cheah,[†] Seonah Kim,[†] Jeffrey T. Miller,[‡] James R. Gallagher,[§] Jesse E. Hensley,[†,#] Joshua A. Schaidle,*[,†] and Daniel A. Ruddy*[,†,#]

[†]National Bioenergy Center, National Renewable Energy Laboratory, Golden, Colorado 80401, United States

[‡]School of Chemical Engineering, Purdue University, West Lafayette, Indiana 47907, United States

[§]Chemical Sciences and Engineering Division, Argonne National Laboratory, Argonne, Illinois 60439, United States

[#]Department of Chemistry, Colorado School of Mines, Golden, Colorado 80401, United States

Supporting Information

ABSTRACT: Cu-based catalysts containing targeted functionalities including metallic Cu, oxidized Cu, ionic Cu, and Brønsted acid sites were synthesized and evaluated for isobutane dehydrogenation. Hydrogen productivities, combined with *operando* X-ray absorption spectroscopy, indicated that Cu(I) sites in Cu/BEA catalysts activate C−H bonds in isobutane. Computational analysis revealed that isobutane dehydrogenation at a Cu(I) site proceeds through a two-step mechanism with a maximum energy barrier of 159 kJ/mol. These results demonstrate that light alkanes can be reactivated on Cu/BEA, which may enable re-entry of these species into the chain-growth cycle of dimethyl ether homologation, thereby increasing gasoline-range (C_{5+}) hydrocarbon yield.

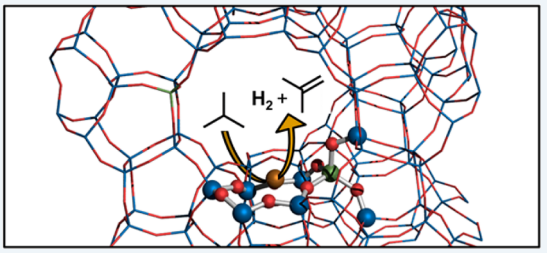

KEYWORDS: *heterogeneous catalysis, C−H activation, dehydrogenation, copper, zeolites*

Zeolite-catalyzed processes represent promising approaches to convert C_1 species (e.g., methanol, dimethyl ether (DME)) from syngas into targeted classes of high-value fuels and chemicals, and a variety of pathways have been developed from the methanol-to-hydrocarbons (MTH) process initially discovered by Mobil Research Laboratories in the 1970s.[1−4] One such process involves the use of large pore acidic zeolites, such as H-BEA, to convert methanol and/or DME to branched C_4−C_7 alkanes, with high selectivity to isobutane and triptane (2,2,3-trimethylbutane).[5,6] This DME homologation process operates at relatively low temperatures (180−220 °C) and pressures (60−250 kPa of DME) compared to other MTH processes. Recent research from our laboratory has demonstrated that the addition of Cu to the BEA zeolite catalyst enables the incorporation of cofed H_2 into the desired products, ultimately resulting in a 2-fold increase in the observed hydrocarbon productivity, relative to unmodified H-BEA.[7]

Improving the carbon efficiency—and, thus, the economic viability—of this process could be achieved by increasing the selectivity to further favor the C_{5+} (gasoline-range) products.[8] Thus, a DME homologation catalyst with dehydrogenation activity offers the opportunity to upgrade the non-gasoline-range C_4 alkane fraction via C−H bond activation and reincorporation of the resulting intermediate or olefin into the chain-growth cycle. Whereas Zn, Ga, and promoted Pt-modified zeolites have been reported to effectively catalyze C−H bond activation in light alkanes (C_1−C_4),[9−13] comparable studies of Cu-modified zeolites are more speculative.[14−17] Previous reports of the strong interaction between Cu(I) sites in MFI and methane or ethane at room temperature suggest that these materials may be capable of activating C−H bonds in light alkanes.[15,16] Kanazirev and Price concluded that cationic Cu sites in Cu/MFI play a key role in propane aromatization at 475 °C.[14] Recently, Itadani et al. hypothesized, based on a combination of infrared spectroscopy experiments and computational modeling, that dimeric Cu(I) sites in ion-exchanged Cu/MFI zeolites may be active for propane dehydrogenation.[17] Grundner et al. reported that trinuclear copper-oxo clusters activate C−H bonds in methane to catalyze the selective oxidation of methane to methanol.[18] Many additional detailed investigations of Cu-modified zeolites have been motivated by the successful application of these materials in the selective catalytic reduction of NO_x and have focused on the speciation of Cu in different zeolite topologies and in the presence of varying NO_x reductants.[19−22] Kefirov et al. specifically studied Cu species in BEA zeolite prepared by ion-exchange and reported that the Cu(II) species completely reduce to Cu(I) under H_2 by 450 °C, although at this high temperature, they note that some small fraction of Cu(0) may

Received: December 17, 2016
Revised: April 6, 2017
Published: April 24, 2017

DOI: 10.1021/acscatal.6b03582
ACS Catal. 2017, 7, 3662−3667

also be formed.[23] Characterization included in our recent report of Cu-modified BEA prepared via incipient wetness impregnation indicated multiple catalytic functionalities, including cationic and metallic Cu sites and Brønsted acid sites.[7] Preliminary temperature-programmed reaction studies, using isobutane dehydrogenation as a simple probe reaction, suggested that these multifunctional materials may activate C−H bonds. Motivated by this initial data, here, we report the synthesis and characterization of multiple Cu-modified catalysts targeting specific catalytic sites of metallic copper, copper oxide, Cu(I) zeolite, Cu(II) zeolite, and Brønsted acid sites. The ability of each site to dehydrogenate isobutane was explored using a combined experimental and computational approach. The active site and corresponding dehydrogenation reaction mechanisms are discussed based on the experimentally observed dehydrogenation activity, characterization using X-ray absorption spectroscopy (XAS), and the results of hybrid quantum mechanics/molecular mechanics (QM/MM) calculations.

To independently investigate the dehydrogenation activity of copper oxide and metallic Cu, we synthesized and tested silica-supported Cu catalysts prepared by incipient wetness impregnation of amorphous silica with an aqueous solution of Cu(II) nitrate to achieve 5.3 wt % Cu. To produce exclusively CuO particles (confirmed by X-ray diffraction; see Figure S1 in the Supporting Information), the material was pretreated in flowing 1% O_2/He at 500 °C for 1 h, yielding a material termed CuO/SiO_2. In contrast, to produce a catalyst with exclusively metallic Cu particles (Figure S1), the oxygen-pretreated CuO/SiO_2 catalyst was subsequently exposed to flowing 2% H_2/He at 300 °C for 1 h, yielding Cu/SiO_2. To determine the dehydrogenation activity of the Brønsted acid sites independently, the proton form of the BEA zeolite, H-BEA, was prepared by calcination of the ammonium form, NH_4−BEA (SiO_2/Al_2O_3 ratio of 27), under flowing air at 500 °C. To explore dehydrogenation at ionic Cu sites, catalysts were prepared using an ion-exchange procedure similar to a reported method.[21,24] The H-BEA zeolite was treated with an aqueous solution of Cu(II) nitrate, isolated by filtration, washed twice with deionized water, and dried at 100 °C overnight. This procedure yielded a material termed IE-Cu/BEA, having 1.8 wt % Cu.

X-ray absorption spectroscopy (XAS) was performed to identify the oxidation state and coordination environment of the ionic Cu species present in the as-prepared IE-Cu/BEA catalyst and following oxidative and reductive pretreatments (see Figure 1A, as well as Figure S2 in the Supporting Information). The X-ray absorption near edge structure (XANES) spectrum of the as-prepared IE-Cu/BEA at room temperature appears almost identical to that of aqueous Cu(II) nitrate.[25] Oxidative treatment of IE-Cu/BEA at 500 °C resulted in the observation of a pre-edge peak at 8978.2 eV, consistent with Cu(II), but different than the hydrated Cu(II) at room temperature (see Table 1 and Figure 1A). Extended X-ray absorption fine structure (EXAFS) analysis revealed a second coordination shell at 2.4−2.5 Å, which is likely due to scattering from Si or Al in the zeolite framework (Figure 1B). No Cu−Cu correlation was found. These data indicate the formation of isolated ion-exchanged Cu(II) sites on the zeolite, termed Cu(II) zeolite sites.

Reductive treatment of ox-IE-Cu/BEA at 300 °C resulted in a significant shift of the XANES edge peak to lower energy, suggesting that Cu(II) had been reduced to Cu(I), consistent

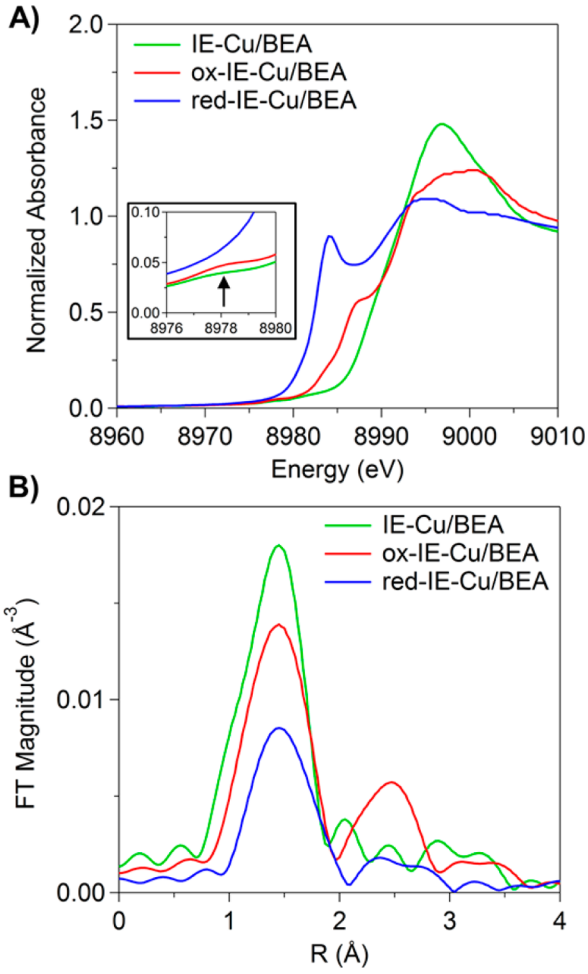

Figure 1. (A) XANES spectra and (B) k^2-weighted Fourier transform magnitude of as-prepared IE-Cu/BEA (Δk = 2.5−10.6 Å^{-1}), oxidized IE-Cu/BEA (ox-IE-Cu/BEA, Δk = 2.5−10.8 Å^{-1}), and oxidized then reduced IE-Cu/BEA (red-IE-Cu/BEA, Δk = 2.5−10.3 Å^{-1}).

with conclusions from a previous temperature-programmed reduction study of Cu/BEA.[23] The EXAFS data indicates a coordination number of 2.3, characteristic of a Cu(I) compound, with an average bond distance of 1.93 Å (Table 1). There is little evidence for a higher shell, suggesting that the Cu(I) ions are mobile, similar to recent reports for Cu-SSZ-13.[22,26] These data demonstrate that catalysts consisting of exclusively Cu(II) zeolite or exclusively Cu(I) zeolite can be accessed from the as-prepared IE-Cu/BEA by varying the pretreatment conditions.

The isobutane dehydrogenation activity of each catalyst was evaluated using a microreactor system. Following oxidative or reductive pretreatment, the catalyst was held at the reaction temperature (300 °C) in flowing He and then exposed to 1% isobutane/Ar at a weight hourly space velocity of 0.20 h^{-1}. The H_2 productivity, as a function of time on stream, representative of the dehydrogenation reaction rate, is presented in Figure 2. The measured H_2 productivities were below the rates corresponding to isobutane dehydrogenation equilibrium at 300 °C (ca. 400 mmol/h). Furthermore, we note that the isobutene product rapidly reacts in subsequent isomerization, oligomerization, and/or alkylation reactions and therefore could not be quantified in the effluent.[27] The productivities of all identified reaction products, as a function of time on

DOI: 10.1021/acscatal.6b03582
ACS Catal. 2017, 7, 3662−3667

Table 1. XANES Pre-edge and Edge Energies, As Well As Coordination Number, Distance, Debye–Waller Factor, and E_0 Shift Obtained from EXAFS Spectra Fitting of an IE-Cu/BEA Catalyst Following Pretreatments

material	treatment	XANES pre-edge energy [eV]	XANES edge energy [eV]	coordination number, N	distance, R [Å]	Debye–Waller factor, $\Delta\sigma^2$ [$\times 10^{-3}$ Å^2]	E_0 [eV]	description
IE-Cu/BEA	as-prepared	8977.9	8988.6	4.1	1.99	1.0	−1.2	hydrated Cu(II)
ox-IE-Cu/BEA	1% O_2/He 500 °C	8978.2	8985.9	3.9	1.91	4.0	−3.5	Cu(II) zeolite
red-IE-Cu/BEA	1% O_2/He 500 °C, 3% H_2/He 300 °C		8982.8	2.3	1.93	4.0	−0.7	Cu(I) zeolite

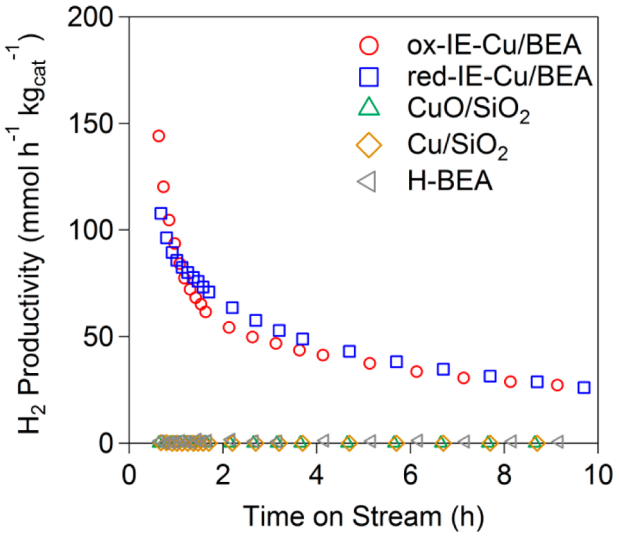

Figure 2. H_2 productivity from 1% isobutane/Ar at 300 °C and 2 atm, as a function of time on stream.

stream, are provided in Figure S3. The H-BEA, CuO/SiO_2, and Cu/SiO_2 clearly exhibited minimal H_2 productivity (Figure 2). The ox-IE-Cu/BEA and red-IE-Cu/BEA displayed comparable H_2 productivities throughout the reaction time, despite the difference in the initial oxidation state of Cu in these catalysts following pretreatment, as determined by *in situ* XAS. These results indicate that ionic Cu sites in BEA zeolite are active for isobutane dehydrogenation at 300 °C, whereas Brønsted acid sites, CuO sites, and metallic Cu sites are not catalytically active.

Operando XAS experiments were performed to determine the oxidation state and stability of the active ionic Cu sites during the isobutane dehydrogenation reaction. Exposing red-IE-Cu/BEA to isobutane led to only small changes in the XANES data (see Figure S4 and Table S1 in the Supporting Information). There is a slight reduction in the number of bonds determined from the EXAFS data, ca. 0.3 fewer, with a small increase in the bond distance from 1.93 Å to 1.98 Å. After ca. 15 min, no further changes were observed in either the XANES or EXAFS spectra, and there was no evidence of the formation of metallic Cu. The minor changes observed could indicate that a small amount (<5%) of remaining Cu(II) was reduced to Cu(I) during isobutane dehydrogenation, or that the Cu(I) species formed in H_2 have a different coordination environment than the Cu(I) formed under isobutane dehydrogenation conditions. The latter explanation is supported by a recent report that utilized CO adsorption and infrared spectroscopy to identify a variety of Cu(I) species (i.e., Cu(I) sites that bind one, two, or three CO molecules) produced from the reduction of Cu(II) in BEA zeolite.[23]

Operando XAS experiments were also performed for the ox-IE-Cu/BEA catalyst (Figure S4 and Table S2 in the Supporting Information). The initial Cu(II) ions were rapidly reduced to Cu(I), with 76% of the Cu(II) ions reduced by 2 min time on stream and 100% of the Cu(II) ions reduced after 2 h time on stream (see Figure 3, as well as Table S2 in the Supporting

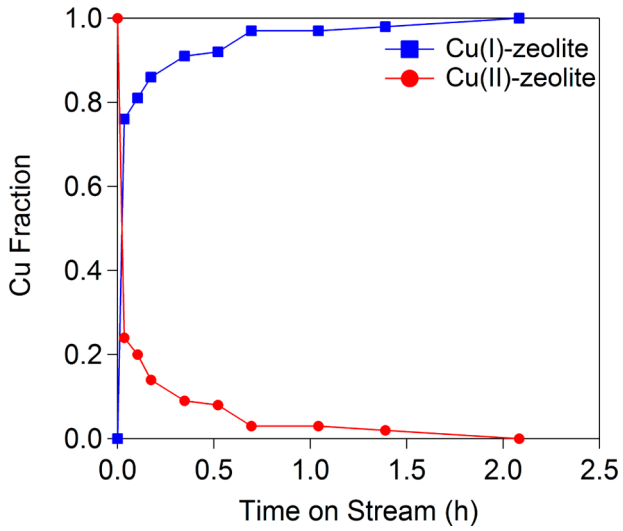

Figure 3. Speciation of ionic Cu in ox-IE-Cu/BEA during isobutane dehydrogenation reaction determined from *operando* XANES.

Information). Note that, after ∼1 h time-on-stream, the XANES spectra and quantitative coordination number and nearest-neighbor distances of the Cu(I) species formed were almost identical to those formed from the red-IE-Cu/BEA catalyst. The Cu(II) species in the ox-IE-Cu/BEA may be reduced by H_2 generated from isobutane dehydrogenation or directly by hydrocarbon molecules. Metallic Cu was not observed under any pretreatment or reaction condition. Therefore, under these isobutane dehydrogenation reaction conditions, regardless of the catalyst pretreatment and corresponding initial oxidation state, there was a rapid reduction of Cu(II) zeolite species to Cu(I) zeolite within 2 h time-on-stream. Thus, the experimentally observed isobutane dehydrogenation activity exhibited by IE-Cu/BEA is attributed to ionic Cu(I) zeolite sites.

To further probe the catalytic activity and reaction mechanism for dehydrogenation at a Cu(I) zeolite site in IE-Cu/BEA, QM/MM calculations were performed using the Gaussian 09 package[28] and a two-layer ONIOM scheme.[29] Additional details of the computational methods, including the impact of the choice of functional and size of the quantum region on the energetics can be found in the Supporting Information (Figure S5). Because of the lack of evidence for Cu–Cu coordination in the EXAFS spectra, the Cu(I) zeolite

DOI: 10.1021/acscatal.6b03582
ACS Catal. 2017, 7, 3662–3667

site was modeled as an isolated Cu(I) site with a single charge-balancing Al substitution in BEA (Figure 4A). Based on a

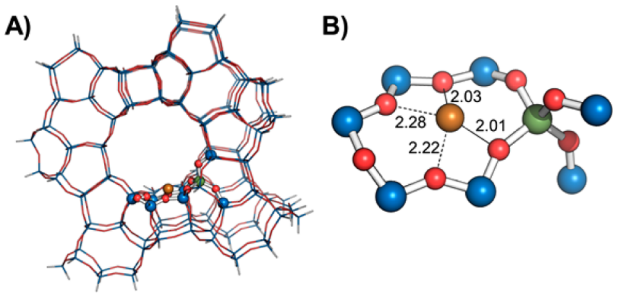

Figure 4. (A) Cu/BEA model with a single Al substitution at a T7 site and the Cu(I) located in the minimum energy location in a six-membered ring of BEA. Wireframe atoms treated with MM and spheres treated with QM. (B) QM region of the Cu/BEA model, with Cu−O distances (Å) indicated. Blue, red, green, and gold spheres represent silicon, oxygen, aluminum, and copper atoms, respectively.

previous report by Vjunov et al. probing the Al distribution in BEA with a similar SiO_2/Al_2O_3 ratio of 25, a T7 site was chosen for the Al substitution site in our model.[30] The minimum energy location of the Cu(I) ion in the BEA zeolite model lies in the six-membered ring associated with the T7 site (Table S3 in the Supporting Information). The Cu(I) ion is located slightly off-center, shifted toward the Al atom (Figure 4B). This Cu(I) site is consistent with the EXAFS data, showing two nearest-neighbor oxygen atoms for Cu(I) zeolite, although the computed bond distances of ca. 2.02 Å are slightly longer, compared to the Cu−O bond distances of 1.98 ± 0.02 Å determined from EXAFS.

The minimum energy reaction mechanism and corresponding energy diagram for the dehydrogenation of isobutane at the most stable six-membered ring Cu(I) site is depicted in Figure 5. This minimum energy pathway was identified based on detailed calculations of numerous hypothesized mechanisms at the six-membered ring site. The energetics were also calculated at the more-open, but less-stable, 12-membered ring site (see Table S4 in the Supporting Information). The calculated barriers are within 15−25 kJ/mol of the barriers reported for the six-membered ring site, indicating that the choice of Cu(I) site has a minor effect on the reported energetics. The charge of the Cu ion was verified by natural population analysis[31] and is reported for each state along the reaction pathway in Table S5 in the Supporting Information. All energies are reported relative to gas-phase isobutane, which adsorbs with a binding strength of 52 kJ/mol at the Cu(I) site. Two reaction mechanisms were identified and these mechanisms differ in the location of the first C−H bond scission in isobutane. The minimum energy pathway involves breaking the first C−H bond at a primary carbon atom (termed primary−tertiary path) and the formation of an O−H bond with the zeolite framework (TS1). The activation energy barrier for this step is 159 kJ/mol. The transition state for the analogous step involving C−H bond scission at the tertiary carbon has a similar activation energy barrier ($\Delta E^{\ddagger}$ = 172 kJ/mol). In the stable intermediate state (INT1), the deprotonated intermediate is bound to the Cu ion and the removed proton is bound to one of the Al−O atoms in the zeolite framework. The second step in the minimum energy pathway is a concerted step in which a second C−H bond breaks at the tertiary carbon, the zeolite(O)−H bond breaks, and a H−H bond forms simultaneously (TS2). The activation

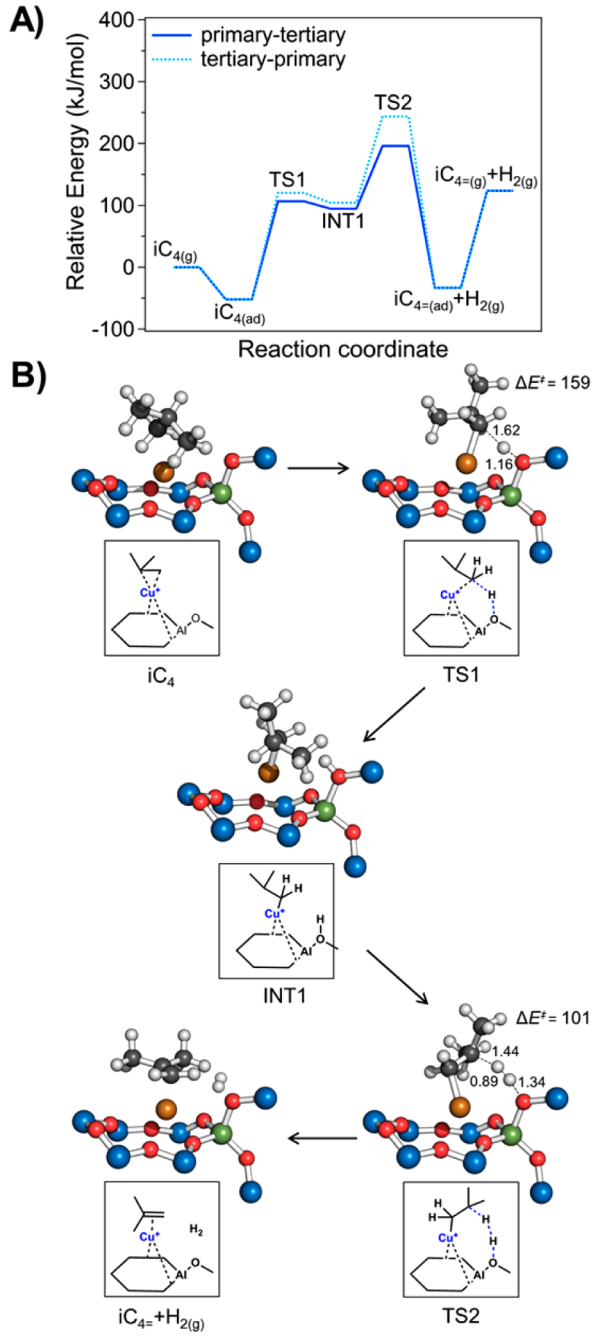

Figure 5. (A) Reaction energy diagram for isobutane dehydrogenation at a Cu(I) site in BEA zeolite. (B) Optimized structures with bond distances (Å) and activation energy barriers ($\Delta E^{\ddagger}$, kJ/mol) for the minimum energy pathway (primary−tertiary path, solid blue line). Structures shown depict only the QM region in QM/MM calculations. Blue, red, white, gray, green, and gold spheres represent silicon, oxygen, hydrogen, carbon, aluminum, and copper atoms, respectively.

energy barrier for this step is 101 kJ/mol. If the first C−H bond scission were to occur at the tertiary carbon, the second step is a similar concerted step, but has a higher activation energy barrier ($\Delta E^{\ddagger}$ = 140 kJ/mol). The structures corresponding to this tertiary−primary reaction mechanism are presented in Figure S6 in the Supporting Information. Regardless of the reaction pathway, the product of the second elementary step is gas-phase H_2 and isobutene adsorbed at the ionic Cu site ($iC_4^{=}$ + H_2) with a binding energy of 154 kJ/mol.

DOI: 10.1021/acscatal.6b03582
ACS Catal. 2017, 7, 3662−3667

This proposed two-step mechanism differs significantly from the light alkane (C_2–C_4) dehydrogenation reaction mechanisms proposed for the GaH_2 site in Ga/MFI,[11] but is quite similar to the proposed mechanism for ethane dehydrogenation at an isolated Zn(II) site in Zn/MFI.[12] The calculated apparent activation energy for isobutane dehydrogenation at a Cu(I) site based on the relative energy surface shown in Figure 5 is 196 kJ/mol. This barrier may be higher than expected to describe the rates observed in our experiments at 300 °C, which is a result that is likely due to limitations of the modeling approach, including the size of the ONIOM structural model and the unaccounted-for electrostatic field of the zeolite. Comparison with the energetics previously reported for isobutane dehydrogenation on Zn- and Ga-modified MFI catalysts with those calculated here for IE-Cu/BEA indicates that one may expect Cu/BEA to be less active for isobutane dehydrogenation, compared to these materials.[11,32]

In summary, Cu-containing catalyst materials were synthesized to target specific catalytic functionalities, namely, metallic copper, copper oxide, Cu(I) zeolite, Cu(II) zeolite, and Brønsted acid sites. Experimental isobutane dehydrogenation reaction studies demonstrated that only the ionic Cu-zeolite catalysts activate C–H bonds in isobutane to produce H_2 under these conditions. Based on *operando* XAS data, it was determined that, regardless of the Cu(I) or Cu(II) speciation in IE-Cu/BEA catalysts following pretreatment, under these isobutane dehydrogenation reaction conditions, the predominant species—and, thus, the active site for C–H bond activation—was Cu(I) zeolite. Computational modeling revealed that the reaction mechanism for isobutane dehydrogenation at a Cu(I) zeolite site in BEA may proceed through a two-step mechanism, with the two consecutive C–H bond-breaking steps having respective activation energy barriers of 159 and 101 kJ/mol, respectively. Thus, as shown for other Lewis acidic metal-modified zeolites, Cu(I) zeolite sites are capable of activating C–H bonds in light alkanes, albeit with higher activation energies. This catalytic functionality may be leveraged in a variety of applications where light alkanes are formed as byproducts, including the potential to upgrade the nonfuel range C_4 alkane products in the Cu/BEA catalyzed DME homologation process to increase carbon efficiency from biomass to fuels.

■ ASSOCIATED CONTENT

Supporting Information

The Supporting Information is available free of charge on the ACS Publications website at DOI: 10.1021/acscatal.6b03582.

Experimental and computational methods, CuO/SiO_2 and Cu/SiO_2 XRD patterns, plot of representative EXAFS data fits, isobutane reaction product plots, *operando* XAS spectra and EXAFS fits, reaction energy diagrams using different functionals, structures for the tertiary–primary pathway, tables of EXAFS data fits for *operando* experiments, relative energies for Cu(I) sites, reaction energetics at different Cu(I)-12-MR sites, calculated atomic charges during isobutane dehydrogenation (PDF)

■ AUTHOR INFORMATION

Corresponding Authors

*E-mail: Joshua.Schaidle@nrel.gov (J. A. Schaidle).
*E-mail: Dan.Ruddy@nrel.gov (D. A. Ruddy).

ORCID

Seonah Kim: 0000-0001-9846-7140
Daniel A. Ruddy: 0000-0003-2654-3778

Author Contributions

The manuscript was written through contributions of all authors. All authors have given approval to the final version of the manuscript.

Notes

The authors declare no competing financial interest.

■ ACKNOWLEDGMENTS

This research was supported by the Department of Energy Bioenergy Technologies Office, under Contract No. DE-AC36-08-GO28308. This work was performed in collaboration with the Chemical Catalysis for Bioenergy Consortium (ChemCatBio), a member of the Energy Materials Network (EMN). Computer time was provided by the NREL High Performance Computing Center. Partial funding for J.R.G. and J.T.M. was provided by Chemical Sciences, Geosciences and Biosciences Division, U.S. Department of Energy, under Contract No. DE-AC0-06CH11357. Use of the Advanced Photon Source is supported by the U.S. Department of Energy, Office of Science, and Office of Basic Energy Sciences, under Contract No. DE-AC02-06CH11357. MRCAT operations are supported by the Department of Energy and the MRCAT member institutions. The authors thank Dr. F. G. Baddour (NREL) for assistance with *in situ* XRD measurements.

■ REFERENCES

(1) Haw, J. F.; Song, W.; Marcus, D. M.; Nicholas, J. B. *Acc. Chem. Res.* **2003**, *36*, 317–326.
(2) Chang, C. D.; Silvestri, A. J. *J. Catal.* **1977**, *47*, 249–259.
(3) Ilias, S.; Bhan, A. *ACS Catal.* **2013**, *3*, 18–31.
(4) Stöcker, M. *Microporous Mesoporous Mater.* **1999**, *29*, 3–48.
(5) Ahn, J. H.; Temel, B.; Iglesia, E. *Angew. Chem., Int. Ed.* **2009**, *48*, 3814–3816.
(6) Hazari, N.; Iglesia, E.; Labinger, J. A.; Simonetti, D. A. *Acc. Chem. Res.* **2012**, *45*, 653–662.
(7) Schaidle, J. A.; Ruddy, D. A.; Habas, S. E.; Pan, M.; Zhang, G.; Miller, J. T.; Hensley, J. E. *ACS Catal.* **2015**, *5*, 1794–1803.
(8) Tan, E. C.; Talmadge, M.; Dutta, A.; Hensley, J.; Snowden-Swan, L. J.; Humbird, D.; Schaidle, J.; Biddy, M. *Biofuels, Bioprod. Biorefin.* **2016**, *10*, 17–35.
(9) Biscardi, J. A.; Iglesia, E. *Catal. Today* **1996**, *31*, 207–231.
(10) Kazansky, V. B.; Subbotina, I. R.; Rane, N.; Van Santen, R. A.; Hensen, E. J. M. *Phys. Chem. Chem. Phys.* **2005**, *7*, 3088–3092.
(11) Pereira, M. S.; Da Silva, A. M.; Nascimento, M. A. C. *J. Phys. Chem. C* **2011**, *115*, 10104–10113.
(12) Pidko, E. A.; Van Santen, R. A. *J. Phys. Chem. C* **2007**, *111*, 2643–2655.
(13) Cortright, R. D.; Hill, J. M.; Dumesic, J. A. *Catal. Today* **2000**, *55*, 213–223.
(14) Kanazirev, V. I.; Price, G. L. *J. Mol. Catal. A: Chem.* **1995**, *96*, 145–154.
(15) Itadani, A.; Sugiyama, H.; Tanaka, M.; Ohkubo, T.; Yumura, T.; Kobayashi, H.; Kuroda, Y. *J. Phys. Chem. C* **2009**, *113*, 7213–7222.
(16) Pidko, E.; Kazansky, V. *Phys. Chem. Chem. Phys.* **2005**, *7*, 1939–1944.
(17) Itadani, A.; Sogawa, Y.; Oda, A.; Ohkubo, T.; Yumura, T.; Kobayashi, H.; Sato, M.; Kuroda, Y. *J. Phys. Chem. C* **2015**, *119*, 21483–21496.
(18) Grundner, S.; Markovits, M. A. C.; Li, G.; Tromp, M.; Pidko, E. A.; Hensen, E. J. M.; Jentys, A.; Sanchez-Sanchez, M.; Lercher, J. A. *Nat. Commun.* **2015**, *6*, 7546.

DOI: 10.1021/acscatal.6b03582
ACS Catal. 2017, 7, 3662–3667

(19) Palomino, G. T.; Bordiga, S.; Zecchina, A.; Marra, G. L.; Lamberti, C. *J. Phys. Chem. B* **2000**, *104*, 8641−8651.
(20) Čapek, L.; Dědeček, J.; Wichterlová, B.; Cider, L.; Jobson, E.; Tokarová, V. *Appl. Catal., B* **2005**, *60*, 147−153.
(21) Kwak, J. H.; Tonkyn, R. G.; Kim, D. H.; Szanyi, J.; Peden, C. H. F. *J. Catal.* **2010**, *275*, 187−190.
(22) Paolucci, C.; Parekh, A. A.; Khurana, I.; Di Iorio, J. R.; Li, H.; Albarracin Caballero, J. D.; Shih, A. J.; Anggara, T.; Delgass, W. N.; Miller, J. T.; Ribeiro, F. H.; Gounder, R.; Schneider, W. F. *J. Am. Chem. Soc.* **2016**, *138*, 6028−6048.
(23) Kefirov, R.; Penkova, A.; Hadjiivanov, K.; Dzwigaj, S.; Che, M. *Microporous Mesoporous Mater.* **2008**, *116*, 180−187.
(24) Bates, S. A.; Verma, A. A.; Paolucci, C.; Parekh, A. A.; Anggara, T.; Yezerets, A.; Schneider, W. F.; Miller, J. T.; Delgass, W. N.; Ribeiro, F. H. *J. Catal.* **2014**, *312*, 87−97.
(25) Cheah, S. F.; Brown, G. E., Jr; Parks, G. A. *J. Colloid Interface Sci.* **1998**, *208*, 110−128.
(26) Goltl, F.; Sautet, P.; Hermans, I. *Catal. Today* **2016**, *267*, 41−46.
(27) Corma, A. *Chem. Rev.* **1995**, *95*, 559−614.
(28) Frisch, M. J.; Trucks, G. W.; Schlegel, G. E.; Scuseria, M. A.; Robb, J. R.; Cheeseman, G.; Scalmani, V.; Barone, B.; Mennucci, G. A.; Petersson, H.; et al. *Gaussian 09, Revision B.01*; Gaussian: Wallingford, CT, 2010.
(29) Vreven, T.; Morokuma, K. *Annu. Rep. Comput. Chem.* **2006**, *2*, 35−51.
(30) Vjunov, A.; Fulton, J. L.; Huthwelker, T.; Pin, S.; Mei, D.; Schenter, G. K.; Govind, N.; Camaioni, D. M.; Hu, J. Z.; Lercher, J. A. *J. Am. Chem. Soc.* **2014**, *136*, 8296−8306.
(31) Glendening, E. D.; Landis, C. R.; Weinhold, F. *J. Comput. Chem.* **2013**, *34*, 1429−1437.
(32) Sun, Y.; Brown, T. C. *Int. J. Chem. Kinet.* **2002**, *34*, 467−480.

DOI: 10.1021/acscatal.6b03582
ACS Catal. 2017, 7, 3662−3667